ARTICLE
Journal of Cellular Biochemistry 111:343–349 (2010)

Journal of Cellular Biochemistry

Calnexin Inhibits Thermal Aggregation and Neurotoxicity of Prion Protein

Wenxi Wang,[1] Rui Chen,[1] Kan Luo,[1] Di Wu,[1] Liqin Huang,[1] Tao Huang,[1] and Gengfu Xiao[1,2*]

[1] *State Key Laboratory of Virology and Modern Virology Research Centre, College of Life Sciences, Wuhan University, Wuhan 430072, PR China*

[2] *State Key Laboratory of Virology, Wuhan Institute of Virology, Chinese Academy of Sciences, Wuhan 430071, PR China*

ABSTRACT

Prion diseases are fatal neurodegenerative disorder associated with the conversion of the cellular isoform of the prion protein (PrP^C) into the infectious scrapie isoform (PrP^{Sc}). Deposition of misfolded prion proteins (PrP) on certain regions of brain can result in prion diseases. As a membrane-bound chaperone of the endoplasmic reticulum (ER), calnexin ensures the proper folding and quality control of newly synthesized proteins. Using purified components in vitro, calnexin associated with many proteins and suppresses their thermal aggregation effectively. We for the first time analyzed PrP-calnexin interaction. The immunoprecipitation, confocal microscope and native polyacrylamide-gel electrophoresis results indicated that calnexin could bind PrP both in vitro and in vivo. The turbidity result showed that calnexin could supress thermal aggregation of PrP. MTT, flow cytometry (FCM) and caspase activity studies demonstrated that calnexin prevent caspase-3-mediated cytotoxicity induced by PrP. These results implied that calnexin is potentially beneficial for the resistance of prion diseases. J. Cell. Biochem. 111: 343–349, 2010.

KEY WORDS: PRION; CALNEXIN; MOLECULAR CHAPERONE; CYTOTOXICITY; APOPTOSIS

Prions cause fatal neurodegenerative diseases including scrapie in sheep, bovine spongiform encephalopathy (BSE) in cattle, Kuru, Gerstmann-Straussler-Scheinker disease (GSS), fatal familial insomnia (FFI), Creutzfeldt-Jakob disease (CJD) and variant Creutzfeldt-Jakob disease (vCJD) in humans [Prusiner, 1997; Aguzzi et al., 2007; Collinge and Clarke, 2007]. A key event in all prion diseases appears to be the supreme structural changes from normal cellular form of prion protein (PrP^C) into the infectious scrapie isoform (PrP^{Sc}). PrP, expressed in many other tissues in addition to the brain, is a highly conserved GPI-anchored N-linked glycoprotein with unknown physiological functions [Harris et al., 1996]. The complete *prnp* gene encodes a signal peptide at the N-terminus from 1–22 aa, a functional domain including 23–231 aa and a GPI-replaceable C-terminal region. PrP contains two *N*-glycan attachment sites at amino acids 181 and 197. PrP in humans also contains an intramolecular disulfide bond (Cys^{179}-Cys^{214}). In some of the prion diseases, the abnormal prion particles recruit normal soluble prion protein (PrP^C) molecules into aggregates, causing endoplasmic reticulum (ER) stress. For example, the patients affected with CJD induced ER stress in the brain [Hetz et al., 2003]. ER stress triggers the unfolding protein response (UPR) associated with the increased expression of chaperones and folding enzymes (e.g., Grp78/BiP, Grp58 and Grp94), which can decrease the aggregation or target the misfolded proteins to proteasome-mediated degradation [Sitia and Braakman, 2003].

As a molecular chaperone in the ER, Calnexin (CNX) ensures the proper folding and quality control of newly synthesized N-linked glycoproteins [Zapun et al., 1997; Ellgaard et al., 1999]. The lectin sites of CNX immediately bind the nascent chains of the newly synthesized N-linked glycoproteins [Hammond et al., 1994; Ware et al., 1995; Spiro et al., 1996]. The lectin site of CNX is specific for a transient oligosaccharide-processing intermediate that possesses a single terminal glucose residue: $Glc_1Man_9GlcNAc_2$ [Wada et al., 1991; Ou et al., 1993; Hammond et al., 1994; Spiro et al., 1996]. CNX can also bind ATP, Ca^{2+}, Zn^{2+} and most importantly, it can bind one of the thiol oxidoreductases in the ER (ERp57). As one of the protein

Additional Supporting Information may be found in the online version of this article.

Grant sponsor: National Natural Science Foundation of China; Grant number: 30970150.

*Correspondence to: Prof. Gengfu Xiao, State Key Laboratory of Virology, Wuhan Institute of Virology, Chinese Academy of Sciences, Wuhan 430071, PR China. E-mail: xiaogf@wh.iov.cn

Received 30 October 2009; Accepted 3 May 2010 • DOI 10.1002/jcb.22698 • © 2010 Wiley-Liss, Inc.
Published online 12 May 2010 in Wiley Online Library (wileyonlinelibrary.com).

disulfide isomerase (PDI), ERp57 facilitates the proper folding of disulfide-bond [Kang and Cresswell, 2002]. CNX binds the unfolding glycoprotein retained in ER and recruits ERp57 to promote the formation of disulfide-bond and isomerization [Williams, 2006].

Some studies have shown that the soluble form of CNX containing an entire ER luminal domain (LD-CNX) is also capable of binding non-glycosylated polypeptides in vitro. Furthermore, LD-CNX can suppress the thermally and chemically induced aggregation and enhance the refolding of polypeptides such as the mitochondrial proteins citrate synthase (CS) and malate dehydrogenase (MDH) [Ihara et al., 1999; Saito et al., 1999].

In this study, we provide the first line of evidence that (1) the ER chaperone CNX can bind PrP; (2) LD-CNX can inhibit the aggregation of the recombinant human full-length prion protein (PrP 23-231); and (3) human CNX could prevent the cytotoxicity induced by $HuPrP^{C}$ (wild-type human PrP, amino acids 1–253).

MATERIALS AND METHODS

PROTEIN EXPRESSION AND PURIFICATION

The human LD-CNX cDNA [Rajagopalan et al., 1994] was cloned into vector pET30a (Novagen) via *Nde*I and *Xho*I restriction sites, resulting in pET30a-LD-CNX plasmid. Plasmid pET30a-PrP 23-231 was constructed in a similar way as described above. After verification by sequencing, the two recombinant plasmids were respectively transformed into *E. coli* BL21 (DE3) strain. The on-column purification and refolding of PrP 23-231 were performed as described previously [Yin et al., 2003]. The concentration of the purified protein was measured using a Bio-Rad protein assay kit (Bio-Rad) with bovine serum albumin as a standard according to the manufacturer's instructions. The Protein solutions were concentrated using a Centricon Plus-20 centrifugal filter devices (10 kDa nominal molecular-mass limit; Millipore).

TURBIDITY ASSAY

PrP 23-231 and LD-CNX were diluted into 10 mM Tris (pH 7.2), 0.15 M NaCl and 2 mM $CaCl_2$. The concentration of PrP 23-231 in all samples was adjusted to 0.2 mg/ml (8 μM). PrP 23-231 was denatured by heating at 65°C for 30 min followed by incubation at temperature of 45°C [Thammavongsa et al., 2005] with different concentrations of LD-CNX (0, 2, 4, 8, and 16 μM) or IgG (16 μM) as control. All samples were added with 0.02% NaN_3 to prevent bacterial growth during the long period of incubation. The turbidity was determined by measuring the absorbance of the samples at every 12 h for a total of 120 h using a UV-Spectrometer (Amersham Ultrospec 3100 pro).

NATIVE POLYACRYLAMIDE-GEL ELECTROPHORESIS (NATIVE-PAGE)

The purified PrP 23-231, LD-CNX, and the mixture of PrP 23-231/LD-CNX at the indicated concentrations were mixed with glycine native sample loading buffer and loaded (15 μl per well) onto a 12% glycine gel with a glycine running buffer, pH 8.8. Gel electrophoresis was carried out with constant 18 mA at 4°C for 1.5 h. The gel was then stained with Coomassie bright blue.

CO-IMMUNOPRECIPITATION AND WESTERN BLOTTING ASSAY

293T cells were grown in DMEM supplemented with 10% fetal bovine serum (FBS). At 70% confluence, cells were co-transfected with a mixture of 6 μg $pcDNA3.1\text{-}HuPrP^{C}$ plasmid and 6 μg pcDNA3.1-CNX using Lipofectamine™ 2000 (Invitrogen). After 48 h of transfection, the cells were resuspended in 50 mM Tris–HCl (pH 7.4), 150 mM NaCl, 1% NP-40, 0.1% SDS (RIPA Lysis buffer). The suspension of the cells was dissolved on ice for 10 min and centrifuged at 15,000*g* for 10 min at 4°C. The supernatants were mixed with anti-CNX 6D195 monoclonal antibody (Santa Cruz) or IgG (as negative control) and Protein A-sepharose beads (Santa Cruz) suspension over night at 4°C. Subsequently, the sepharose beads were precipitated at 1,000*g* for 5 min and washed with PBS for three times. The bound complexes were separated by 10% SDS–PAGE and transferred onto a polyvinylidene difluoride (PVDF) membrane. PrP or CNX was detected by using anti-PrP 8H4 (Sigma), anti-CNX 6D195 (Santa Cruz) monoclonal antibodies. Immunodetection was followed by incubation with the relative alkaline phosphatase-conjugated secondary antibody. In order to further confirm the endogenous interaction between PrP and CNX, we performed co-immunoprecipitation assay on non-transfected SK-N-SH cells. Immunodetection was followed by incubation with the relative horseradish peroxidase-conjugated secondary antibody.

CONFOCAL MICROSCOPY

pDsRed-CNX and pEGFP-PrP were transiently co-transfected into Human neuroblastoma cells (SK-N-SH) using Lipofectamine™ 2000 (Invitrogen). After 24 h, images were acquired using Revolution XD confocal microscopy (Andor). GFP-PrP signal was excited with a 488 nm helium-neon laser and a 525 nm band-pass filter for emission. pDsRed-CNX signal was excited with 488 nm laser, and a 625 nm band-pass filter was used for emission.

MTT ASSAY

SK-N-SH cells were grown in MEM supplemented with 10% fetal bovine serum (FBS). The cells were cultured in flasks and were distributed into a 96-well polystyrene plate at a concentration of 10^4 cells/100 μl medium per well. At 70% confluence, cells were transfected or co-transfected with different concentrations of pcDNA3.1, pcDNA3.1-CNX and $pcDNA3.1\text{-}HuPrP^{C}$ plasmids with Lipofectamine™ 2000 transfection reagent (Invitrogen). After 48 h of transfection, the MTT [3-(4, 5-dimethylthiazol-2-yl)-2,5-diphenyl-2H-tetrazolium bromide] (Sigma) was added to the culture medium at final concentration of 1 mg/ml and incubated at 37°C for 4 h. The supernatant was removed and each well was added with 200 μl of DMSO to dissolve the formazan product. Optical density was measured at 595 nm using a Microplate Spectrophotometer (TECAN Genios spectra FLUOR plus). Each sample was performed in duplication of at least four wells, and each experiment was repeated at least three times.

FLOW CYTOMETRY ASSAY

Apoptosis was assayed by Annexin-FITC/PI (propidium iodide) staining following the manufacturer's instructions (Bender MedSystems). Briefly, after 48 h of transfection, cells were collected and washed in cold PBS. After cells were resuspended in 200 μl 1×

binding buffer, annexinV-FITC (1×) and PI (5 μg/ml) were added in the dark and incubated at room temperature for 15 min. After incubation, 500 μl of 1× binding buffer was added to each sample, and cells were analyzed by flow cytometry (Beckman Coulter Epics XL).

CASPASE-3 ACTIVITY

Colorimetric assay of caspase-3 activity. After 48 h of transfection, the cells were collected and washed with 0.01 M phosphate-buffered saline (PBS, pH 7.2). After centrifugation, caspase-3 colorimetric assay was performed with a caspase-3/CPP32 colorimetric assay kit (BioVision) following the manufacturer's instructions on Microplate Spectrophotometer (TECAN Genios spectra FLUOR plus).

Western blot assay of caspase-3 activity. After 48 h of transfection, the cells were resuspended in 50 μl RIPA Lysis buffer. The cells were dissolved on ice for 10 min and added 10 μl 6× SDS–PAGE loading buffer. The samples were separated by 10% SDS–PAGE and transferred onto a PVDF membrane. Caspase-3 and β-actin were detected by using anti-Caspase-3 (Santa Cruz) and anti-β-actin (Santa Cruz) polyclonal antibodies.

RESULTS

INTERACTION BETWEEN PrP23-231 AND LD-CNX BOTH IN VITRO AND IN VIVO

To test whether PrP 23-231 and LD-CNX interact with each other in vitro, native PAGE was performed. In the native-PAGE (Fig. 1A, lane 1), PrP 23-231, with net positive charges, migrated up and out of the gel under the native electrophoresis conditions, and thus, no band could be detected in the gel. In the same condition, LD-CNX migrated down in the gel due to its net negative charges (Fig. 1A, lane 2). The mixture of LD-CNX and PrP 23-231 showed two bands in the gel (Fig. 1A, lane 3). The upper band was in the same position as the purified LD-CNX (Fig. 1A, lane 2) and the lower one was expected to be the complex formed by the association of PrP 23-231 with LD-CNX (Fig. 1A, lane 3). In order to confirm whether the lower band indeed represents the complex of the PrP 23-231 and LD-CNX, we analyzed the mixture of PrP 23-231 and LD-CNX at different ratios by N-PAGE (Fig. 1B). The concentrations of PrP 23-231 were constant and the intensity of the complex band was increased with increasing concentrations of LD-CNX (from lane 2 to lane 6). These data indicated that PrP 23-231 was associated with LD-CNX in vitro and formation of complex was dependent on the concentration of LD-CNX. We next performed co-immunoprecipitation to confirm the interaction between PrP and CNX in mammalian cells. Plasmids pcDNA3.1-HuPrP^{C} and pcDNA3.1-CNX were co-transfected into 293T cells. The protein complexes extracted from transfected cells were immunoprecipitated with anti-CNX mAb, and blotted by anti-PrP mAb and anti-CNX mAb. PrP was found to be co-immunoprecipitated with CNX (Fig. 1C). We also performed co-immunoprecipitation to further confirm the endogenous interaction between PrP and CNX in SK-N-SH cells. The fusion proteins extracted from untransfected cells were immunoprecipitated with anti-CNX mAb. PrP was found to be co-immunoprecipitated with CNX (Fig. 1D). These results confirmed that CNX interacted with PrP in vivo. In order to further confirm the

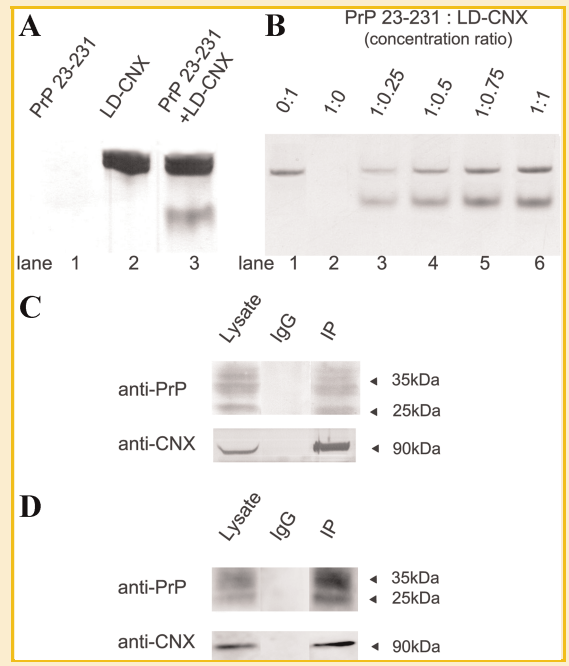

Fig. 1. The association of HuPrP with CNX in vitro and in vivo was detected by Native-PAGE and immunoprecipitation, respectively. A: Lane 1, only PrP 23-231 with net positive charges was loaded and showed no band. Lane 2, LD-CNX carrying net negative charges was loaded. Lane 3, the reaction complex of PrP 23-231 and LD-CNX showed two bands. The upper band was in the same position as purified LD-CNX, and the lower one was expected to be the complex of PrP 23-231 and LD-CNX. B: With increasing concentrations of LD-CNX (from lane 2 to lane 6: 0, 5, 10, 15, 20 μM), the intensity of complex bands increased. Constant concentration of PrP 23-231 (20 μM) was used in this experiment. C: Immunoprecipitation was used to detected the association of HuPrP^{C} with CNX in mammalian cells. The lysate from the 293T co-transfected with pcDNA3.1-HuPrP^{C} and pcDNA3.1-CNX was immunoprecipitated by anti-CNX mAb and blotted by anti-PrP mAb and anti-CNX mAb. IgG was used to serve as a control. D: Immunoprecipitation was used to detected the endogenous association of PrP with CNX in mammalian cells. The lysate from the SK-N-SH cells was immunoprecipitated by anti-CNX mAb and blotted by anti-PrP mAb and anti-CNX mAb. IgG was used to serve as a control.

interaction between CNX and PrP, confocal microscopy was used to study the two proteins in vivo. We constructed two plasmids of CNX and PrP fused with fluorescent proteins (pDsRed-CNX and pEGFP-PrP), and then co-transfected them into SK-N-SH cells. As shown in Figure 2, PrP and CNX were co-localized in the ER. These results confirmed that CNX interacted with PrP in mammalian cells.

INHIBITION OF THERMAL AGGREGATION OF PrP 23-231 BY LD-CNX

To assess whether CNX is capable of functioning as a molecular chaperone in vitro, we prepared a soluble form of CNX consisting of its entire ER luminal segment (LD-CNX) and tested its ability to inhibit the thermal aggregation of PrP 23-231. PrP 23-231 was denatured by heating at 65°C for 30 min. The denatured PrP 23-231 was diluted into solutions containing various concentrations of LD-CNX or IgG (as a negative control) and incubated at 45°C to induce aggregation. As shown in Figure 3, PrP 23-231 alone aggregated following a lag period of first 2 days and then aggregated rapidly.

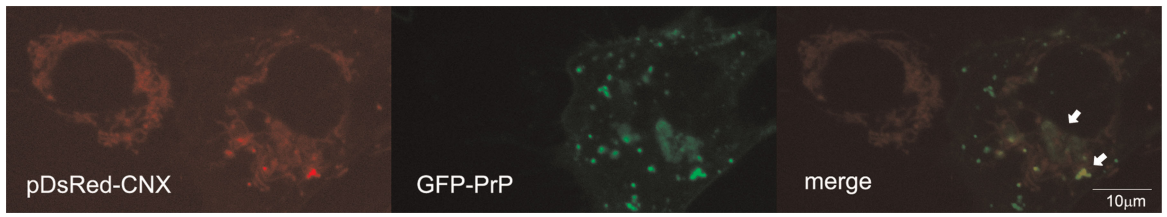

Fig. 2. Co-localization of CNX and PrP in transfected cells. CNX and PrP fusion proteins had red and green colors, respectively, co-localization of proteins was demonstrated by arrowheads in the merge panel. [Color figure can be viewed in the online issue, which is available at wileyonlinelibrary.com.]

Consistent with a molecular chaperone function, LD-CNX effectively inhibited the aggregation of PrP 23-231 in a concentration-dependent manner. In contrast, an equivalent amount of IgG added as a control had no effect on the aggregation of PrP 23-231.

CNX INHIBITS PrP-INDUCED CYTOTOXICITY

We further performed MTT assay to investigate if the cytotoxicity of $HuPrP^C$ could be inhibited by CNX. Human neuroblastoma cells were transfected individually with plasmids pcDNA3.1, pcDNA3.1-$HuPrP^C$ and pcDNA3.1-CNX, co-transfected with both pcDNA3.1-$HuPrP^C$ and pcDNA3.1-CNX, or un-transfected as blank control (Fig. 4A). The results showed that the viability of the cell over-expressing $HuPrP^C$ was decreased remarkably, while the viability of the cells over-expressing both CNX and $HuPrP^C$ was comparable to blank untransfected cells as well as the cells transfected with pcDNA3.1 or pcDNA3.1-CNX (Fig. 4A). When the concentrations of pcDNA3.1-$HuPrP^C$ plasmid were constant, the viability of the cell was increased with increasing concentration of pcDNA3.1-CNX (Fig. 4B). These results indicated that CNX can inhibit the $HuPrP^C$-induced cytotoxicity in a concentration-dependent manner.

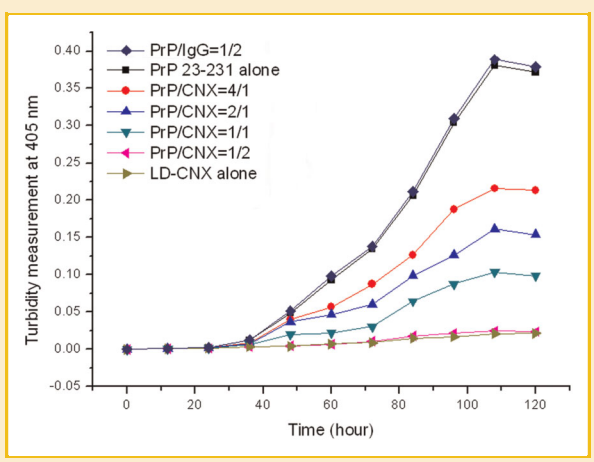

Fig. 3. LD-CNX suppressed the thermal aggregation of PrP 23-231. PrP 23-231 (8 μM) was incubated at 45°C in the presence of various concentrations of LD-CNX (0–16 μM) or IgG (16 μM), and aggregation was monitored by UV-Spectrometer at 405 nm. [Color figure can be viewed in the online issue, which is available at wileyonlinelibrary.com.]

CNX INHIBITS PrP-INDUCED APOPTOSIS

To investigate whether CNX could inhibit the cell apoptosis induced by $HuPrP^C$ in SK-N-SH cells, we performed Annexin V-FITC/PI staining and flow cytometry analyses. The percentage of apoptotic cells was 4.8% and 4.1%, respectively, when the cells were transfected with pcDNA3.1-CNX and pcDNA3.1. The untransfected cells had an apoptotic cell percentage of 3.7% (Fig. 5A–C). As shown from Figure 5D to I, the concentration of pcDNA3.1-$HuPrP^C$ plasmid were constant, the percentage of apoptotic cells were reduced with the increasing concentration of pcDNA3.1-CNX. When the cells were transfected with pcDNA3.1-$HuPrP^C$ alone, the percentage of apoptotic cells reached 17.9% (Fig. 5D). When the concentration ratio of pcDNA3.1-$HuPrP^C$ to pcDNA3.1-CNX were 1:0.2, 1:0.4, 1:0.6, 1:0.8, and 1:1, the percentage of apoptotic cells were 13.6%, 9.9%,6.9%, 5.8%, and 5.0%, respectively (Fig. 5E–I). These results suggested that CNX can suppress the apoptosis caused by $HuPrP^C$.

CNX PREVENT CASPASE-3-MEDIATED CELL APOPTOSIS INDUCED BY PrP

To investigate the mechanism of the inhibition of CNX in $HuPrP^C$ induced apoptosis, caspase-3 colorimetric assay was used to evaluate the quantity of active caspase-3. Caspase-3 was a cysteine protease, and the activation of caspase-3 indicated that cells entered an apoptotic pathway. According to Figure 6A, the activated caspase-3 increased remarkably when transfected $HuPrP^C$ alone, which indicated apoptosis. When fixed the quantity of $HuPrP^C$, the activated caspase-3 was decreased along with the increasing of transfected CNX. We further performed western blot to measure the activation of caspase-3, the decrease of the precursor of caspase-3 (pro-caspase-3). As shown in Figure 6B, the activated caspase-3 was decreased along with the increasing CNX, meanwhile the levels of inactive pro-caspase-3 was increased. These results showed that CNX could prevent caspase-3-mediated cell apoptosis which induced by PrP.

DISCUSSION

We demonstrated for the first time that the PrP interacts with CNX in vitro and in mammalian cells. Previous studies show that the lectin chaperone CNX has two mechanisms of association with glycoproteins: (1) lectin-binding or (2) lectin and polypeptide binding [Ware et al., 1995; Danilczyk and Williams, 2001]. The PrP 23-231 expressed in *E. coli* was not glycosylated and thus, the interaction of

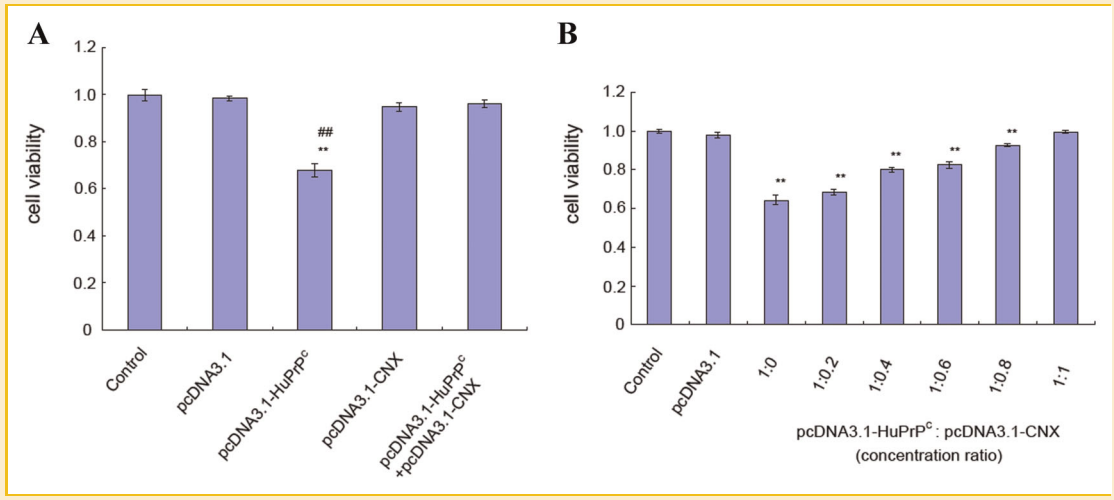

Fig. 4. A: Influences of the transfected HuPrP^C on the cell viability in the presences or absence of CNX. MTT assay was performed after 48 h of transfection. The viability of the cells transfected HuPrP^C was statistically different to those transfected with pcDNA3.1 ($^{**}P < 0.01$), or co-transfected with both HuPrP^C and CNX ($^{\#\#}P < 0.01$). B: Dose-response effects of transfection with CNX. "**" indicates the statistical difference between the cells transfected with HuPrP^C alone and those transfected with increasing concentration of CNX ($P < 0.01$). [Color figure can be viewed in the online issue, which is available at wileyonlinelibrary.com.]

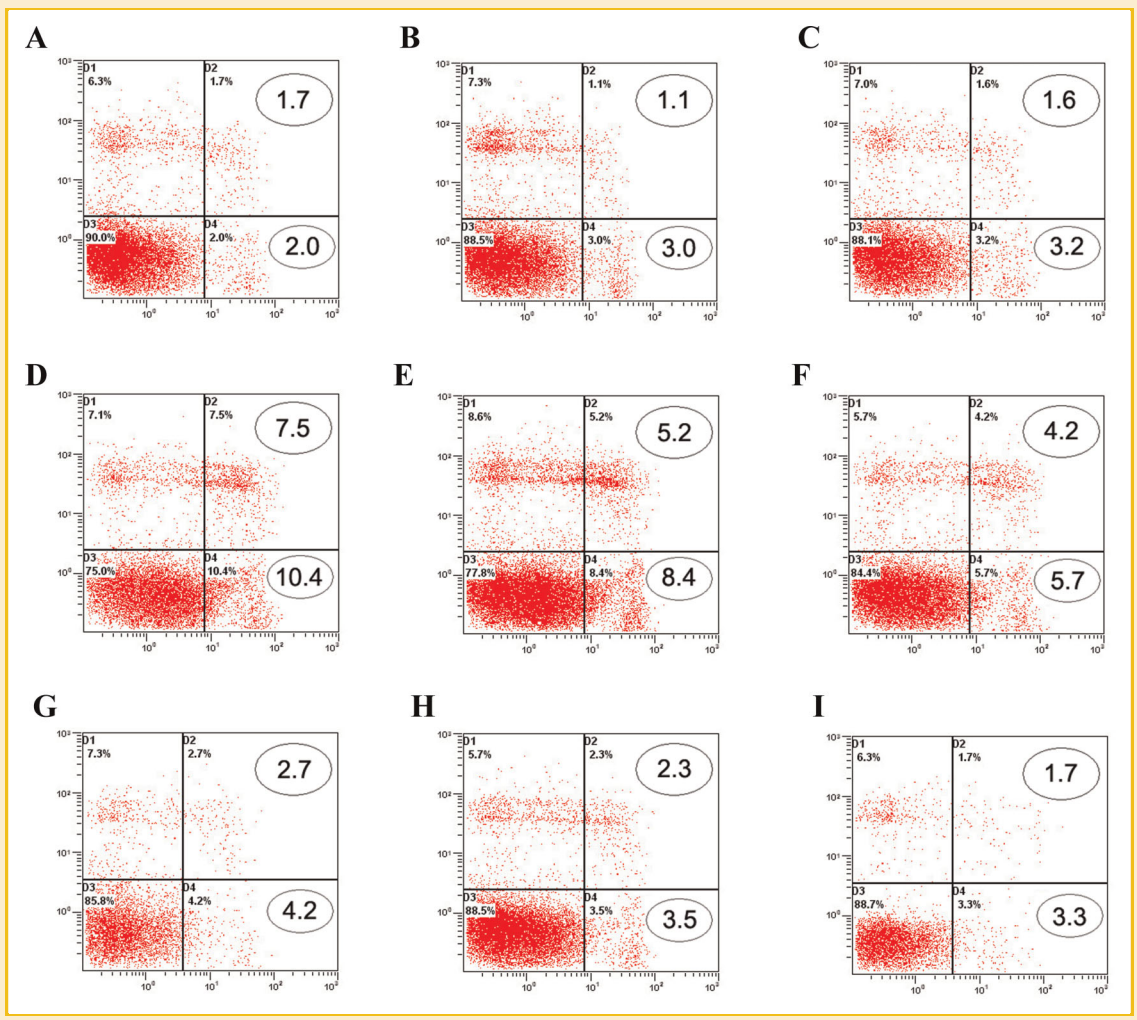

Fig. 5. Flow cytometry analysis of SK-N-SH cell apoptosis after transfection. X-axis indicated the numbers of Annexin V-FITC stained cells. Y-axis indicated the numbers of PI stained cells. The percentage of the overall population of apoptosis in D2 and D4 quadrant were given in circles. A: Untransfected control cells. B: Cells transfected with pcDNA3.1. C: Cells transfected with pcDNA3.1-CNX. D: Cells transfected with pcDNA3.1-HuPrP^C. E–I: The concentration of pcDNA3.1-HuPrP^C plasmid were constant (0.5 μg) and the concentration of pcDNA3.1-CNX was increased (0.1, 0.2, 0.3, 0.4, and 0.5 μg). [Color figure can be viewed in the online issue, which is available at wileyonlinelibrary.com.]

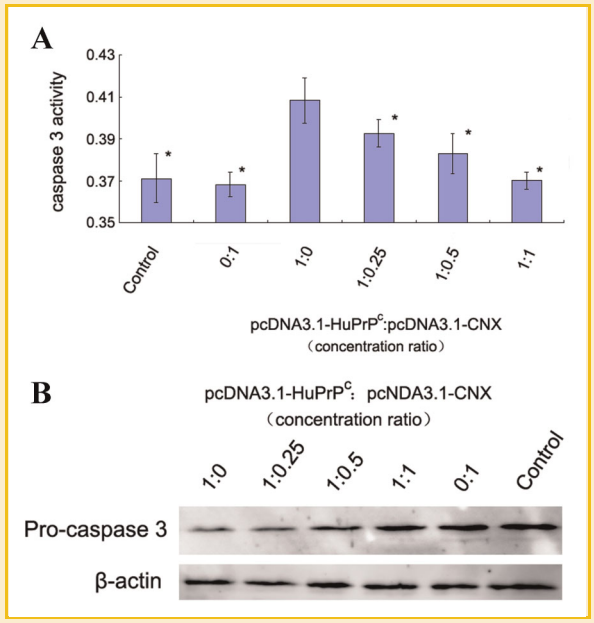

Fig. 6. The caspase-3 activity in SK-N-SH cells after transfection. A: Caspase-3 activity in transfected cells was measured by caspase colorimetric assay kit. The caspase-3 activity of cells transfected with $HuPrP^C$ alone (1:0) was statistically different to those normal control, transfected with CNX alone (0:1), co-transfected with both $HuPrP^C$ and increasing concentration of CNX (from 1:0.25 to 1:1) ($^*P < 0.05$). B: Pro-caspase-3 in transfected cells was measured by western blot. SK-N-SH cells were transfected with CNX, $HuPrP^C$, and co-transfected with $HuPrP^C$ and increasing concentration of CNX. Cell lysates were then separated on 10% SDS-PAGE and probed with antibody against caspase-3. β-Actin was used as a loading control. [Color figure can be viewed in the online issue, which is available at wileyonlinelibrary.com.]

PrP 23-231 with LD-CNX maybe dependent on polypeptide binding site. Some studies have indicated that LD-CNX can discriminate between unfolded and native substrate proteins, and be associated with unfolded proteins by its hydrophobic surface in vitro [Hartl, 1996; Saito et al., 1999]. Our previous studies suggested that PrP 23-231 differs remarkably from most of the other globular proteins because its native conformation contains a large unstructured and flexible segment (residues 23-126) [Sun et al., 2005], which is easily recognized by chaperons. The tendency of PrP^{Sc} aggregation in aqueous solution depends on the hydrophobic surface exposure [Barducci et al., 2005]. In this study, we demonstrated that PrP can interact with LD-CNX. We hypothesize that binding of PrP with LD-CNX may occupy the hydrophobic sites of PrP 23-231, which prevents PrP self-polymerization. If sufficient LD-CNX is provided, the thermal aggregation may be inhibited completely.

Wild-type PrP is a plasma membrane protein and translocates to the cell surface *via* the ER. Like other proteins transported through the ER, misfolded PrP is retrograde transported to the cytosol for degradation by proteasomes. However, if neuroblastoma cells over-expressing wild-type PrP are treated with proteasome inhibitors, the un-degradated cytosolic wild-type PrP is accumulated and caused neurotoxicity [Ma and Lindquist, 2001; Yedidia et al., 2001; Ma et al., 2002]. In this study, we found that the viability of human neuroblastoma cells (SK-N-SH) transfected $HuPrP^C$ alone were decreased remarkably. We speculated that the over-expressed $HuPrP^C$ was accumulated in the cytoplasm because the folding capacity of the ER was compromised. Previous studies indicated that PrP could be deglycosylated when it was retrograde transported to cytoplasm, and accumulation of unglycosylated species were more likely to be converted into a PrP^{Sc}-like form [Lehmann and Harris, 1997; Suzuki et al., 2000] which induced caspase-3-mediated cell death [Hetz and Soto, 2003]. As an ER resident chaperone, CNX can refold or target misfolded proteins for degradation [Ellgaard and Helenius, 2003; Hirsch et al., 2004]. We hypothesize that the expression of CNX increases proper folding of over-expressed $HuPrP^C$ in ER and decreases the content of cytosolic $HuPrP^C$, which consequently reduces the PrP-induced cytotoxicity.

ER is known as a factory where approximately one-quarter of the membranous and secreted proteins are structurally maturated [Hebert and Molinari, 2007]. Correspondingly, the ER provides an optimized environment for high concentrations of general chaperones. Accumulation of misfolded proteins in ER has been associated with many neurodegenerative disorders [Soto, 2003]. The ER chaperone disulfide isomerase, Grp58, can interact with PrP^{Sc}, protect cells against PrP^{Sc}-induced toxicity and decrease the rate of caspase-12 activation [Hetz et al., 2005]. BiP, as an ER chaperone, can also bind and degrade mutant PrP through the proteasomal pathway [Jin et al., 2000]. Our findings indicated that another ER chaperone, CNX, can not only suppress the aggregation of PrP in vitro, but also inhibit the cytotoxicity caused by over-expression of PrP. We reasoned that CNX may have clinical benefits in prion-related diseases and other protein conformation-associated diseases such as Alzheimer's, Parkinson's and Huntington's diseases [Soto and Estrada, 2008], and other disorders especially resulted from protein misfolding and accumulation.

ACKNOWLEDGMENTS

We are grateful to Dr. Micheal B. Brenner for kindly providing the plasmids of human lumenal domain calnexin and full-length calnexin. This work was supported by National Key Scientific Program (973)-Nanoscience and Nanotechnology (No. 2006CB933100), grant from National Natural Science Foundation of China (No. 30970150) and program for Changjiang Scholars and Innovative Research Team in University (No. IRT 0745).

REFERENCES

Aguzzi A, Heikenwalder M, Polymenidou M. 2007. Insights into prion strains and neurotoxicity. Nat Rev Mol Cell Biol 8:552–561.

Barducci A, Chelli R, Procacci P, Schettino V. 2005. Misfolding pathways of the prion protein probed by molecular dynamics simulations. Biophys J 88:1334–1343.

Collinge J, Clarke AR. 2007. A general model of prion strains and their pathogenicity. Science 318:930–936.

Danilczyk UG, Williams DB. 2001. The lectin chaperone calnexin utilizes polypeptide-based interactions to associate with many of its substrates in vivo. J Biol Chem 276:25532–25540.

Ellgaard L, Helenius A. 2003. Quality control in the endoplasmic reticulum. Nat Rev Mol Cell Biol 4:181–191.

Ellgaard L, Molinari M, Helenius A. 1999. Setting the standards: Quality control in the secretory pathway. Science 286:1882–1888.

Hammond C, Braakman I, Helenius A. 1994. Role of N-linked oligosaccharide recognition, glucose trimming, and calnexin in glycoprotein folding and quality control. Proc Natl Acad Sci USA 91:913–917.

Harris DA, Gorodinsky A, Lehmann S, Moulder K, Shyng SL. 1996. Cell biology of the prion protein. Curr Top Microbiol Immunol 207:77–93.

Hartl FU. 1996. Molecular chaperones in cellular protein folding. Nature 381:571–579.

Hebert DN, Molinari M. 2007. In and out of the ER: Protein folding, quality control, degradation, and related human diseases. Physiol Rev 87:1377–1408.

Hetz C, Soto C. 2003. Protein misfolding and disease: The case of prion disorders. Cell Mol Life Sci 60:133–143.

Hetz C, Russelakis-Carneiro M, Maundrell K, Castilla J, Soto C. 2003. Caspase-12 and endoplasmic reticulum stress mediate neurotoxicity of pathological prion protein. EMBO J 22:5435–5445.

Hetz C, Russelakis-Carneiro M, Walchli S, Carboni S, Vial-Knecht E, Maundrell K, Castilla J, Soto C. 2005. The disulfide isomerase Grp58 is a protective factor against prion neurotoxicity. J Neurosci 25:2793–2802.

Hirsch C, Jarosch E, Sommer T, Wolf DH. 2004. Endoplasmic reticulum-associated protein degradation–one model fits all? Biochim Biophys Acta 1695:215–223.

Ihara Y, Cohen-Doyle MF, Saito Y, Williams DB. 1999. Calnexin discriminates between protein conformational states and functions as a molecular chaperone in vitro. Mol Cell 4:331–341.

Jin T, Gu Y, Zanusso G, Sy M, Kumar A, Cohen M, Gambetti P, Singh N. 2000. The chaperone protein BiP binds to a mutant prion protein and mediates its degradation by the proteasome. J Biol Chem 275:38699–38704.

Kang SJ, Cresswell P. 2002. Calnexin, calreticulin, and ERp57 cooperate in disulfide bond formation in human CD1d heavy chain. J Biol Chem 277: 44838–44844.

Lehmann S, Harris DA. 1997. Blockade of glycosylation promotes acquisition of scrapie-like properties by the prion protein in cultured cells. J Biol Chem 272:21479–21487.

Ma J, Lindquist S. 2001. Wild-type PrP and a mutant associated with prion disease are subject to retrograde transport and proteasome degradation. Proc Natl Acad Sci USA 98:14955–14960.

Ma J, Wollmann R, Lindquist S. 2002. Neurotoxicity and neurodegeneration when PrP accumulates in the cytosol. Science 298:1781–1785.

Ou WJ, Cameron PH, Thomas DY, Bergeron JJ. 1993. Association of folding intermediates of glycoproteins with calnexin during protein maturation. Nature 364:771–776.

Prusiner SB. 1997. Prion diseases and the BSE crisis. Science 278:245–251.

Rajagopalan S, Xu Y, Brenner MB. 1994. Retention of unassembled components of integral membrane proteins by calnexin. Science 263:387–390.

Saito Y, Ihara Y, Leach MR, Cohen-Doyle MF, Williams DB. 1999. Calreticulin functions in vitro as a molecular chaperone for both glycosylated and non-glycosylated proteins. EMBO J 18:6718–6729.

Sitia R, Braakman I. 2003. Quality control in the endoplasmic reticulum protein factory. Nature 426:891–894.

Soto C. 2003. Unfolding the role of protein misfolding in neurodegenerative diseases. Nat Rev Neurosci 4:49–60.

Soto C, Estrada LD. 2008. Protein misfolding and neurodegeneration. Arch Neurol 65:184–189.

Spiro RG, Zhu Q, Bhoyroo V, Soling HD. 1996. Definition of the lectin-like properties of the molecular chaperone, calreticulin, and demonstration of its copurification with endomannosidase from rat liver Golgi. J Biol Chem 271: 11588–11594.

Sun G, Guo M, Shen A, Mei F, Peng X, Gong R, Guo D, Wu J, Tien P, Xiao G. 2005. Bovine PrP^{C} directly interacts with alphaB-crystalline. FEBS Lett 579:5419–5424.

Suzuki T, Park H, Hollingsworth NM, Sternglanz R, Lennarz WJ. 2000. PNG1, a yeast gene encoding a highly conserved peptide:N-glycanase. J Cell Biol 149:1039–1052.

Thammavongsa V, Mancino L, Raghavan M. 2005. Polypeptide substrate recognition by calnexin requires specific conformations of the calnexin protein. J Biol Chem 280:33497–33505.

Wada I, Rindress D, Cameron PH, Ou WJ, Doherty JJ II, Louvard D, Bell AW, Dignard D, Thomas DY, Bergeron JJ. 1991. SSR alpha and associated calnexin are major calcium binding proteins of the endoplasmic reticulum membrane. J Biol Chem 266:19599–19610.

Ware FE, Vassilakos A, Peterson PA, Jackson MR, Lehrman MA, Williams DB. 1995. The molecular chaperone calnexin binds Glc1Man9GlcNAc2 oligosaccharide as an initial step in recognizing unfolded glycoproteins. J Biol Chem 270:4697–4704.

Williams DB. 2006. Beyond lectins: The calnexin/calreticulin chaperone system of the endoplasmic reticulum. J Cell Sci 119:615–623.

Yedidia Y, Horonchik L, Tzaban S, Yanai A, Taraboulos A. 2001. Proteasomes and ubiquitin are involved in the turnover of the wild-type prion protein. EMBO J 20:5383–5391.

Yin SM, Zheng Y, Tien P. 2003. On-column purification and refolding of recombinant bovine prion protein: Using its octarepeat sequences as a natural affinity tag. Protein Expr Purif 32:104–109.

Zapun A, Petrescu SM, Rudd PM, Dwek RA, Thomas DY, Bergeron JJ. 1997. Conformation-independent binding of monoglucosylated ribonuclease B to calnexin. Cell 88:29–38.